Source-structure tradeoff in Noise Tomography

SHRAVAN HANASOGE (*hanasoge@princeton.edu*)

Department of Geosciences, Princeton University

QUEST 2013: ABSTRACT

Cross correlations of microseismic oscillations excited by oceanic activity, recorded by seismometers, are used to infer structural properties of Earth. The sources of these oscillations are typically localized, resulting in anisotropic illumination of the crust. Here, we attempt to characterize the impact of the tradeoff between source and structure by posing a 2-D inverse problem where an arbitrary distribution of sources illuminates the heterogeneous medium. We use the adjoint method to compute noise cross correlation kernels (e.g., Gizon & Birch 2002, Tromp et al. 2010, Hanasoge et al. 2011, Hanasoge 2013) for travel-time, amplitude, and waveform-difference measurements. We also compute classical structure kernels for these measurements and compare them with the corresponding noise kernels.

Introduction

Terrestrial seismic noise is generated at a range of temporal frequencies, by human activity, storms, oceanic wave microseisms (e.g., Longuet-Higgins, 1950). Seismic noise is as used as a compelling alternative to earthquake tomography to image the crust. Most importantly, it enables the study of temporal variations of the crust (e.g., Zaccarelli et al., 2011) and volcanoes (Brenguier et al., 2007). Under controlled circumstances, such as when the source distribution is uniform, representation theorems (e.g., Fleury et al., 2010) demonstrate that cross correlations may be written as a modulation of Green's function between the stations. This allows for a classical treatment of noise measurements. However, Earth noise is typically anisotropic and in such a scenario, Green's functions along some source-station paths are weighted more strongly than others and the elegant correspondence may be lost. Here, we attempt to characterize some of the tradeoffs incurred in an anisotropically illuminated medium.

The model

We consider a 2-D medium where wave propagation is described by

$$\rho\,\partial_t^2\mathbf{v} + \rho\,\Gamma\,\partial_t\mathbf{v} - \boldsymbol{\nabla}(\rho c^2\boldsymbol{\nabla}\cdot\mathbf{v}) = \mathbf{f}(\mathbf{x},t), \tag{1}$$

where $\mathbf{v}$ is the wave velocity, ρ the density of the medium, c the wavespeed, Γ the attenuation (measured in inverse units of time), $\boldsymbol{\nabla}$ the covariant spatial derivative, t time, ∂_t the derivative with respect to time, $\mathbf{f}$ the source and $\mathbf{x}$ the spatial coordinate. In order to analyze the interplay between source and structure when inverting for the latter, we consider a heterogeneous medium, but a specific form for which an exact solution is known. The geometry is shown in Figure 1, where a disc-shaped perturbation is placed at the center of the domain.

Figure 1 shows a medium that has two sets of properties, c_d, ρ_d, Γ_d being the wavespeed, density and attenuation respectively associated within the disc and c_e, ρ_e, Γ_e the corresponding properties of the exterior. An incident wave, whose acoustic potential is denoted by $\phi_{\rm inc}$, propagates toward the heterogeneity and is scattered by it, resulting in reflected $\phi_{\rm ref}$ and internal $\phi_{\rm int}$ waves. By construction, the reflected wave only propagates in the external region whereas the internal wave describes the field within the disc.

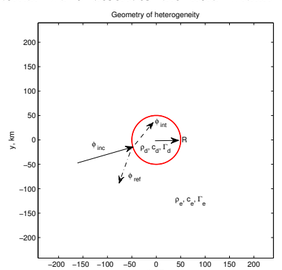

(Figure 1. Pictorial description of the geometry of the problem.)

Analytical Solution

The governing differential equation (1) is solved locally in the disc and in the exterior and the solutions are then matched at the boundary of the two regions. A circular disc-like heterogeneity renders the matching tractable by analytical means, and hence the choice for the geometry in Figure 1. The solution is locally expanded in cylindrical harmonics in each of the regions with matching conditions given by continuity of the normal component velocity and pressure (e.g., Gizon et al., 2006). We introduce an acoustic potential ϕ

$$\mathbf{v} = \frac{1}{\rho}\boldsymbol{\nabla}\phi, \tag{2}$$

such that the differential equation is transformed to

$$\partial_t^2\phi + \Gamma\,\partial_t\phi - c^2\nabla^2\phi = S(\mathbf{x},t). \tag{3}$$

For a temporally stochastic and spatially stationary and uncorrelated distribution of sources S, a situation relevant in some cases to Earth ambient noise, it may be shown that the expected cross correlation is connected to Green's functions of the medium thus

$$\mathcal{C}(\mathbf{x}_i,\mathbf{x}_j,\omega) = \int d\mathbf{x}'\, G^*(\mathbf{x}_i,\mathbf{x}';\omega)\, G(\mathbf{x}_j,\mathbf{x}';\omega)\, S(\mathbf{x}')\, \mathcal{P}(\omega), \tag{4}$$

where $\mathcal{P}(\omega)$ is the temporal power spectral distribution of the sources, $S(\mathbf{x}')$ the spatial distribution of sources, $G(\mathbf{x},\mathbf{x}',\omega)$ is Green's function measured at point $\mathbf{x}$ due to a source at $\mathbf{x}'$. The quantity $\mathcal{C}$ is the cross correlation of signals measured at receivers $\mathbf{x}_i, \mathbf{x}_j$.

Figure 2 displays an example cross correlation and the reference measured at a pair of stations separated by a distance of 120 km, where the wavespeed of the medium is 3 km/s. The stations are placed symmetrically across the origin, on the x-axis of Figure 1. The wavespeed anomaly within the disc is +10%, with no density or attenuation contrasts. The horizontal axis is time lag measured in seconds. The positive and negative branches correspond to positive and negative time lags respectively. Travel times measured in each branch are denoted by τ^+ and τ^-. The average and difference of these two travel times are termed mean and difference times respectively

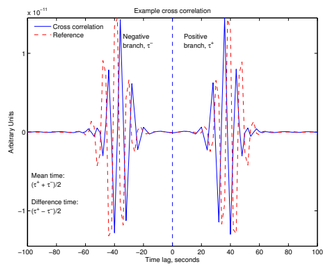

(Figure 2. Sample cross correlation)

Measurements & Kernels

As in Figure 2, the cross correlation function has two branches, the positive-lag branch ($t > 0$) and the negative-lag branch ($t < 0$). Thus two travel times may be extracted from each cross correlation, and we denote τ^+ as the travel time obtained from the positive branch and τ^- as the travel time associated with the negative branch. In the inversion, we will use *mean and difference travel times*, which are defined as (e.g., Gizon & Birch, 2002)

$$\tau^m = \frac{\tau^+ + \tau^-}{2}, \qquad \tau^d = \frac{\tau^+ - \tau^-}{2}. \tag{5}$$

The energy of the cross correlation is given by (e.g., Hanasoge, 2013)

$$\varepsilon = \sqrt{\frac{1}{T}\int dt\, w(t)\, \mathcal{C}^2}, \tag{6}$$

and the waveform difference is $w(t)(\mathcal{C}_{\rm ref} - \mathcal{C})$, where $w(t)$ is a windowing function. Thus we have four measurements from a cross correlation: *mean travel time*, *difference travel time*, *energy*, and *waveform difference*. With 'data', choices for measurements and starting model, we are ready to compute finite frequency kernels. A general computational adjoint theory for noise kernels was described by Tromp et al. (2010); here, since we restrict ourselves to considering a uniform starting model, we can afford to study a simpler problem. The travel-time, amplitude and waveform-difference misfit functionals are given by

$$\chi = \frac{1}{2}\sum_{ij}\tau_{ij}^2, \tag{7}$$

$$\chi^\varepsilon = \frac{1}{2}\sum_{ij}\left[\ln\left(\frac{\varepsilon_{ij}^{\rm ref}}{\varepsilon_{ij}}\right)\right]^2, \tag{8}$$

$$\chi^{\rm w} = \frac{1}{2}\sum_{ij}\int dt\, w(t)\,(\mathcal{C}-\mathcal{C}_{\rm ref})^2.$$

(Figure 3. Example wavespeed (top two rows) and impedance (bottom two rows) kernels for energy, waveform difference, mean and difference travel-time measurements for a station pair located 120 km apart. The stations are placed symmetrically with respect to the origin on the x-axis of Figure 1. . The integral of the difference travel time kernel is zero and is not sensitive to wavespeed anomalies. The energy kernel is interesting in that it does not have a 'doughnut hole' in the center, which the travel-time kernels evidently possess. Waveform differences are also sensitive to the underlying anomaly, also appearing to not possess a 'hole'. The source distribution is uniform in this case, resulting in strong symmetries about the bisector between and line joining the two stations.)

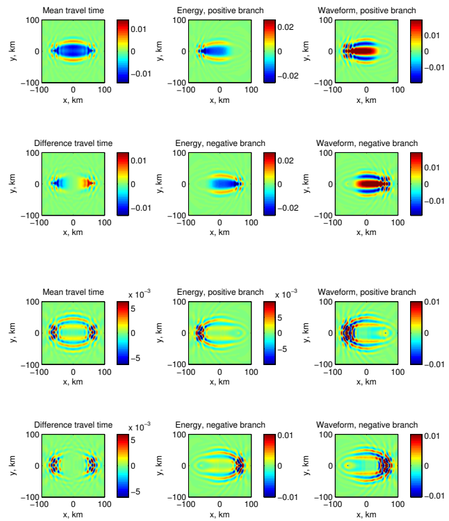

The kernels are designed to address non-dimensional quantities and are connected to the variation of the misfit (for a given measurement) thus

$$\delta\chi = \int d\mathbf{x}\, K_c(\mathbf{x})\,\delta\ln c + K'_\rho(\mathbf{x})\,\delta\ln\rho + K_\Gamma(\mathbf{x})\,\delta\ln\Gamma, \tag{9}$$

where K_c, K'_ρ, K_Γ are the wavespeed, impedance and attenuation kernels respectively

Stations and Geometry

(Figure 4. We consider a network of 24 stations (marked by diamonds) surrounding a wavespeed anomaly (inner red ring). Two cases, with isotropic (left) and anisotropic (right) source distributions, illuminate the medium. The ray-path coverage of the network is excellent within the central disc, suggesting that the eventual inversion will likely be good.)

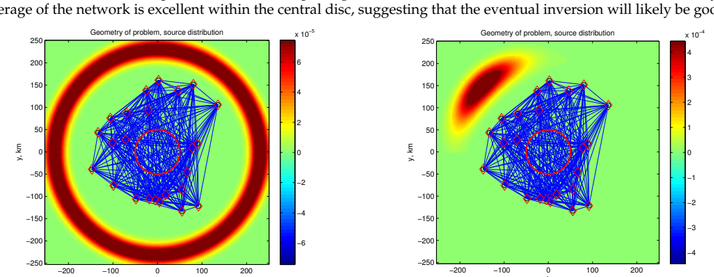

(Figure 4. Stations, source distribution and ray coverage.)

Sum of event kernels

For all the problems, the starting structure model is a homogeneous uniform medium. We explore the following variants here:

1. Only wavespeed perturbation (+10%), true source distribution is uniform (Fig. 4, left), starting source distribution model = true source distribution,
2. Only wavespeed perturbation (+10%), true source distribution is non-uniform (Fig. 4, right), starting source distribution model = uniform,
3. Only wavespeed perturbation (+10%), true source distribution is non-uniform (Fig. 4, right), starting source distribution model = true source distribution

(Figure 5. Sum of all event kernels, i.e., the sum over sensitivity kernels between every point-pair. The sum of all event kernels, in some ways, is the inversion, since it is the gradient of the entire misfit functional. There four functions that we have imperfect knowledge of and that we wish to invert for: wavespeed, impedance, attenuation, and source distribution. We have four different measurements, mean and difference travel times, energies and waveform misfit. The true model contains only a wavespeed perturbation of +10% within the central disc. **Left**: This is a best-case scenario (1). **Right, top**: Wavespeed update zoomed in (left panel) and treating noise measurements as if they were classical (right panel). **Right, bottom**: Panel, left to right, in order: cases (2), (3) and the classical treatment.

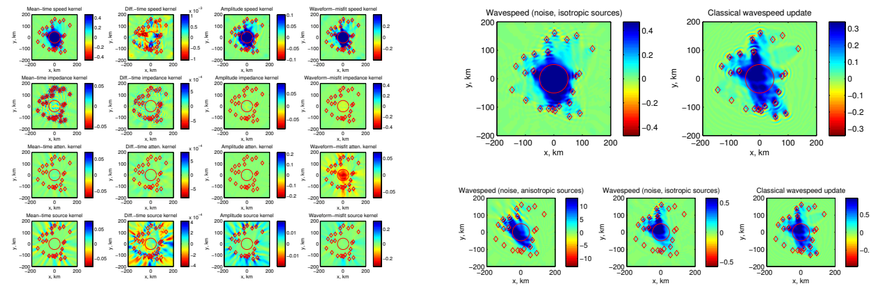

(Figure 5. Sum of event kernels)

Summary

Through the construction of a 2-D toy problem for which an analytical solution exists, we attempt to study the source-structure tradeoff in the inverse problem. Based on amplitude, travel time and waveform difference measurements, we compute updates for a uniform starting model. Some preliminary conclusions:

- Anisotropic source distributions decrease the fidelity of inversions when not modeled. Taking this into account can speed up inversions and decrease uncertainties.
- Applying classical (earthquake) adjoint theory to noise measurements does appear to work although there are some differences between the two inversions.
- An algorithm to speed up noise inversions may involve treating noise measurements classically in early iterations, and subsequently treating them formally correctly à la Tromp et al. (2010).
- Attenuation requires accurate information about the source distribution; it is much more sensitive to the source model than wavespeed.

References

⇒ Longuet-Higgins 1950. A Theory of the Origin of Microseisms. RSLPT A, 243, 1.
⇒ Gizon & Birch 2002. Time-Distance Helioseismology: The Forward Problem for Random Distributed Sources. ApJ, 571, 966.
⇒ Gizon, Hanasoge & Birch 2006. Scattering of Acoustic Waves by a Magnetic Cylinder: Accuracy of the Born Approximation. ApJ, 643, 549.
⇒ Brenguier et al. 2007. 3-D surface wave tomography of the Piton de la Fournaise volcano using seismic noise correlations. GRL, 34, 2305.
⇒ Tromp, Luo, Hanasoge Peter 2010. Noise Cross-Correlation Kernels. GJI, 183, 791.
⇒ Fleury et al. 2010. General Representation Theorem for Perturbed Media and Application to Green's Function Retrieval for Scattering Problems. GJI, 183, 1648.
⇒ Hanasoge, Birch, Gizon Tromp 2011. The Adjoint Method Applied to Time-Distance Helioseismology. ApJ, 738, 100.
⇒ Zaccarelli et al. 2011. Variations of Crustal Elastic Properties During the 2009 L'Aquila Earthquake Inferred from Cross-correlations of Ambient Seismic Noise. GRL, 38, 24304.
⇒ Hanasoge 2013. The Influence of Noise Sources on Cross-correlation Amplitudes. GJI, 192, 295.